

Supporting Information

Controllable Heterogeneity in Supramolecular Hydrogel

Atsuomi Shundo,^{*a} Keiko Mizuguchi,^b Misao Miyamoto,^{cd} Masahiro Goto,^{ae}
Keiji Tanaka^{*abe}

^aDepartment of Applied Chemistry, ^bDepartment of Automotive Science, ^dArt, Science and Technology Center for Cooperative Research, ^eCenter for Future Chemistry, Kyushu University, 744 Motoooka, Nishi-ku, Fukuoka 819-0395, Japan, and ^cNissan Chemical Industries, Ltd., 3-7-1 Kandanishiki Cho, Chiyoda-ku, Tokyo 101-0054, Japan

Contents

1. Materials.....	S2
2. Micro Rheology.....	S2
2-1. Optical configuration of optical tweezers	
2-2. Evaluation of spring constant for optical trap	
2-3. Measurements	
3. Bulk Rheology.....	S7
4. Fluoresence Spectroscopy.....	S8
5. Fourier-Transform Infrared Spectroscopy.....	S9
6. Reference.....	S10

1. Materials

N-palmitoyl-Gly-Gly-Gly-His trifluoroacetate (**PalG₃H**) was synthesized by employing standard Fmoc chemistry.¹ Water, after distillation with an Autostill WG33 (Yamato Scientific Co., Ltd.) and successive deionization with a Milli-Q Lab (Millipore), was used for the gel formation. The specific resistance of the purified water was greater than 18 MΩ cm. For microrheological studies, an aqueous dispersion of polystyrene microspheres containing fluorescence probes, the so-called Fluoresbrite Yellow Green Microsphere, with a concentration of 2 wt% was purchased from Polysciences Inc. The diameter of the microspheres was 1.08 ± 0.02 μm. Also, for fluorescence spectroscopy, 8-anilidonaphthalene-1-sulfonate sodium salt (**ANS**) purchased from Tokyo Kasei Chemical Co. was used as received. Deuterated water (D₂O) and dimethyl sulfoxide (DMSO-*d*₆) purchased from MERCK & Co. Inc. and Cambridge Isotope Laboratories, Inc., respectively, were used for Fourier transform infrared (FT-IR) spectroscopy.

2. Micro Rheology

2-1. Optical configuration of optical tweezers. Fig. S1 represents our setup of optical tweezers based on an inverted microscope, Nikon ECLIPSE Ti, with an NA1.30 oil-immersion objective lens. The light generated by a Nd:YAG laser with a wavelength of 1064 nm (Furukawa Electric Co., Ltd.) was used to trap probe particles. The laser beam was sinusoidally oscillated at a frequency of 1.0 Hz *via* a piezo-driven mirror, which was controlled by a function generator (Modul ENV 40, Piezosystem jena, GmbH). A halogen lamp illuminated the sample and a CCD camera (DS-Qi1MS, Nikon Instech Co., Ltd.) acquired images of the trapped particles in the sample with a frame rate of 60 Hz. NIS-Elements AR-3.2 Software (Nikon Instech Co., Ltd.) was used for tracking the particle oscillation. The amplitude was determined by curve-fitting analysis. The displacement of a particle was detected as a function of time by a quadrant photodiode (OP711, SENTEC Co., Ltd.). Signals from the function generator and the photodiode were introduced into a lock-in amplifier (7260, EG&G Co., Ltd.) to obtain the phase lag between them.

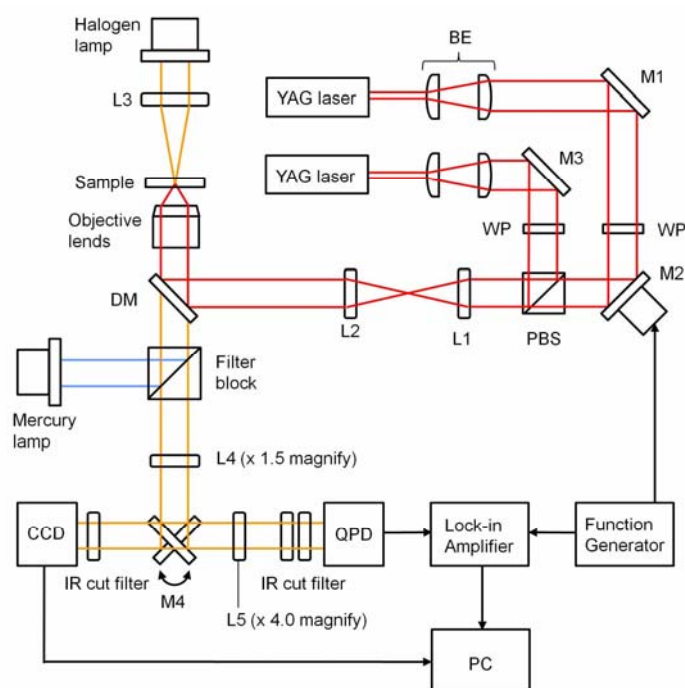


Figure S1 Optical configuration of optical tweezers; BE: beam expander, M1, 3 and 4: mirrors, M2: piezo-controlled mirror, WP: wave plate, PBS: polarizing beam splitter, L1-5: lens, CCD: charge-coupled device, QPD: quadrant-photodiode, PC: personal computer.

2-2. Evaluation of spring constant for optical trap. Since the laser intensity has a Gaussian profile, Hooke's law with an apparent spring constant, k_{OT} , is applied as a model to represent the force of the optical trap. The k_{OT} value in our measurement was determined by a hydrodynamic method^{2,3} based on Stokes and Hooke's laws:

$$k_{OT} = 6\pi\eta av / d \quad (1)$$

where η is the viscosity of the medium, a is the particle radius, v is the velocity of the solution flow and d is the distance between the particle and the centre of the laser beam.

To evaluate the spring constant for the optical trap, we used an ideal media, namely water, containing the same type of particles. A particle was optically trapped with a given laser power and then the water was caused to flow by moving a substage.² When the water flow which alternated in direction was applied, as shown in Figure S2,a, the particle position shifted, showing the approximately square wave response shown in Figure S2,b. The step height in the response of the particle position corresponded to twice the distance of the particle from the centre of the laser beam, $2d$. The distance, d together with the

known parameters, η , a and v gave a k_{OT} value at a given laser power. After confirming that the k_{OT} value was linearly proportional to the laser power, the linear coefficient was $0.130 \text{ pN (nm W)}^{-1}$, enabling us to find the k_{OT} value at a laser power. Given that a spring constant so obtained retains even in our gel and sol samples thanks to its low concentration, the viscoelastic moduli were here obtained.⁴

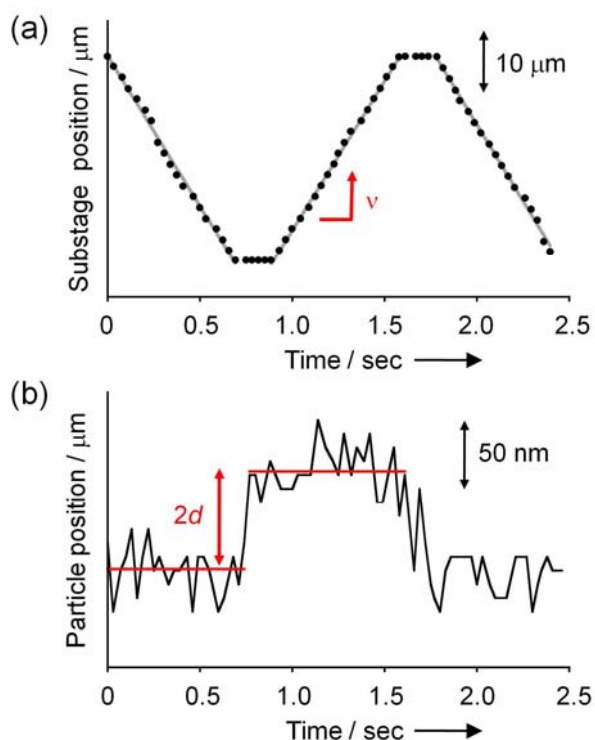


Figure S2 Substage motion to generate a water flow which alternated in direction (a) and the corresponding displacement of a probe particle (b).

2-3. Measurement. PalG₃H with a weight of 6 mg and the particle latex solution with a volume of 2 μL were well-dispersed into 3 mL of water by sonication for 10 min, and then, this dispersion was kept for 10 min at 363 K or 333 K, to prepare gel and sol. The resultant hot solution was poured into a glass bottom dish (MATSUNAMI GLASS Inc. Ltd.). The sample was aged for 1 hour at room temperature after being protected with a cover glass. Figure S3 shows the time dependence of the particle position driven by Brownian motion. The extent to which a particle can move is in the order of water, sol and gel.

A particle in the gel was optically trapped and then was sinusoidally oscillated with the amplitude in the range of $0.077 - 2.6 \mu\text{m}$ at 1.0 Hz . Figure S4 shows the amplitude difference between laser and particle movements as a function of the laser amplitude. Each value was normalized by the corresponding laser amplitude. The difference decreased as the laser amplitude increased. This indicates that the fibrous network in the gel was in part broken by the particle movement and the extent of the destruction became more significant with increasing laser amplitude. However, this should not affect our central point in this work that there exists the heterogeneity in the fibrous network of the gel sate.

During the oscillation of a particle in the gel, it was found that another particle was oscillated without optical trap. As shown in panel (a) of Figure S5, the center-to-center distance between the two particles (particles I and II) was $12.5 \mu\text{m}$. When the particle I was sinusoidally oscillated with the amplitude of $2.71 \mu\text{m}$ at 1.0 Hz (in Figure S5b), the particle II followed that motion, as shown in panel (c) of Figure S5. The amplitudes for the particle II and the phase lag between the particle I and II were $0.18 \pm 0.005 \mu\text{m}$ and 11° , respectively. The laser beam should not directly cause the movement of particle II because the beam radius on a focus plane was approximately $0.85 \mu\text{m}$. Thus, it is likely that the movement of particle I is propagated to the particle II through the fibril and/or its network. Such a phenomenon was ever observed for the particles in the sol.

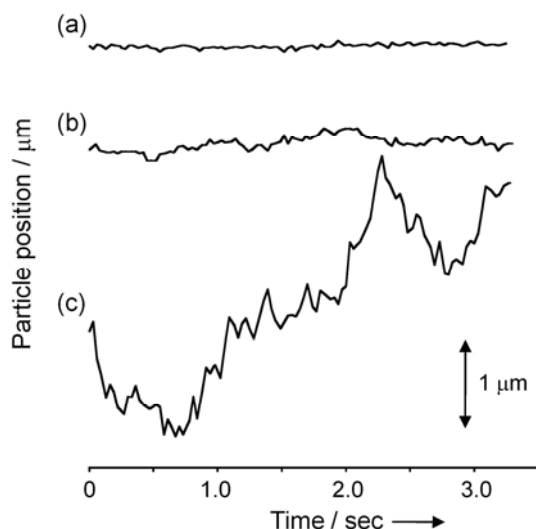


Figure S3 Typical Brownian motions of a probe particle in gel (a), sol (b) and water (c).

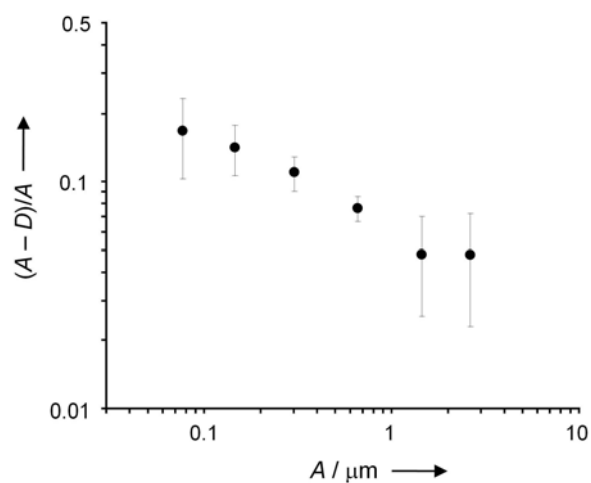


Figure S4 Relation between laser-amplitude and the amplitude dependence between laser and particle movements, $(A - D)/A$, where A and D are the amplitudes of sinusoidal movements of the laser and particle, respectively.

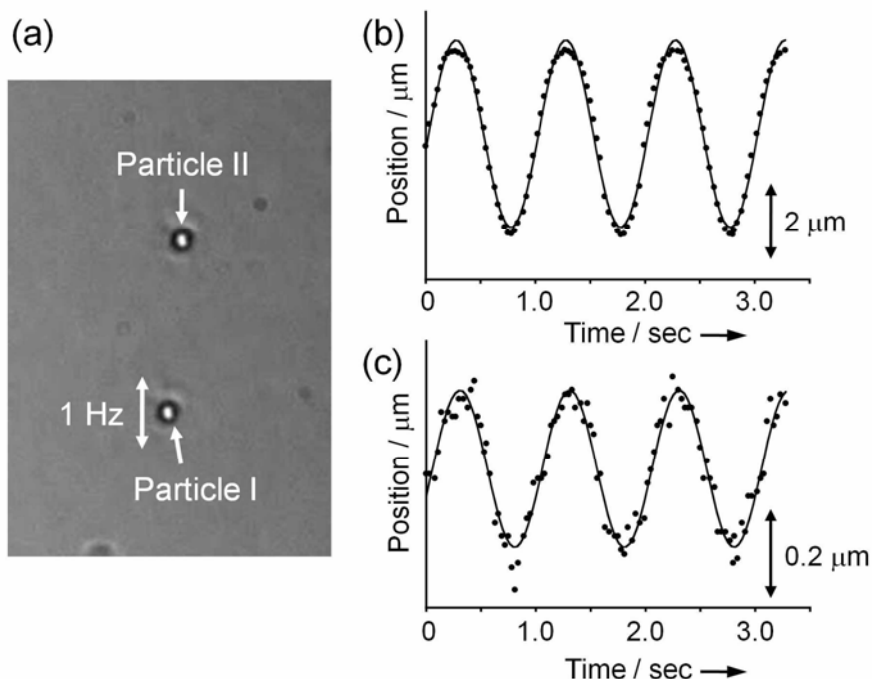


Figure S5 Optical microscopic image of the particles dispersed into the gel (a) and sinusoidal movement of the particles I (b) and II (c) at a frequency of 1.0 Hz.

3. Bulk Rheology

Rheological measurements of the gel were performed by an AR-G2 rheometer (TA instruments Co. Ltd.). Each of the samples was held between the sample stage and a cone-typed plate with a diameter of 60 mm and a tilt angle of 1° . The Wet papers with water were laid around the sample to prevent water evaporation from the sample during the measurement.

The 0.2 wt% aqueous suspension of **PalG₃H** pre-kept at 363 K was mounted on a sample stage, which was controlled in temperature at 298 K, and then was aged for 20 min, resulting in the completion of the gelation, as shown in Figure S6. Then, a frequency sweep was performed at a strain amplitude of 0.3 %, which was in the linear viscoelastic regime. Figure S7 shows the frequency dependence of the viscoelastic functions, such as dynamic storage and loss moduli, $\tan \delta$ and viscosity at 298 K. Both G' and G'' were essentially independent of frequency and G' was larger than G'' at a given frequency. Also, they did not cross-over, even in the low frequency region. This behavior is a signature that the material is a rigid gel.⁵

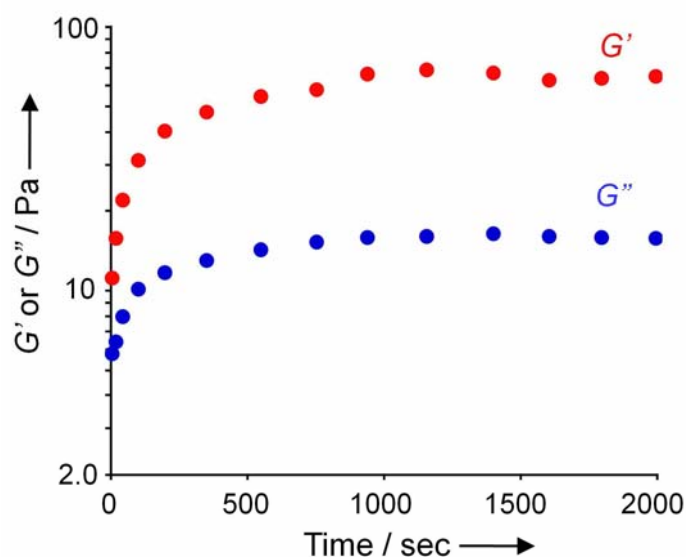


Figure S6 Time dependence of viscoelastic functions for the 0.2 wt% **PalG₃H** aqueous solution pre-kept at 363 K right after letting it age at 298 K.

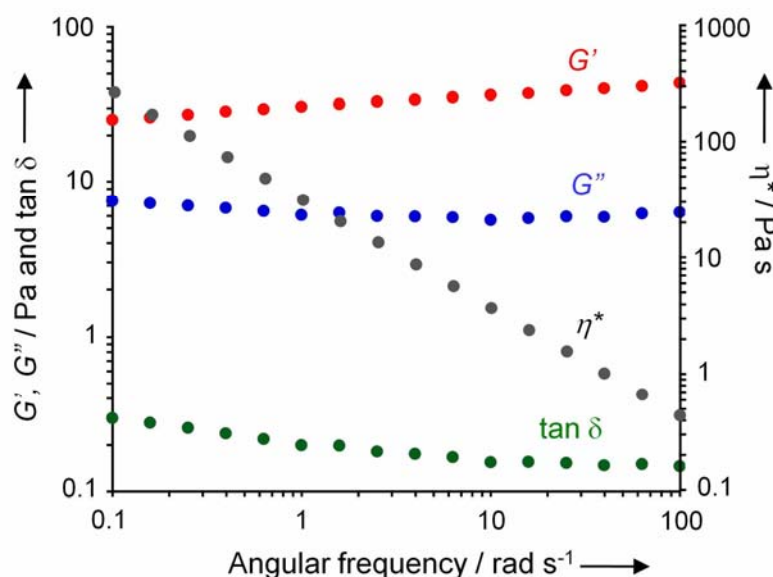


Figure S7 Frequency dependence of viscoelastic moduli for the 0.2 wt% **PalG₃H** solution well-aged at 298 K.

4. Fluorescence Spectroscopy

A methanol solution of **ANS** with a concentration of 10^{-3} M was prepared. This solution with a volume of 3 μ l was added into 3 mL water, which was placed in a quartz cell with a path-length of 10 mm. **PalG₃H** with a weight of 6 mg was well-dispersed into the mixture by sonication for 10 min, and then the dispersion was heated in water for 10 min at 363 K or 333 K, to prepare a gel and sol, respectively. After aging it for 1 hour at 298 K, fluorescence spectra were recorded using a F-4500 Spectrophotometer (Hitachi High-Technologies Co.). Figure S8 shows fluorescence spectra of **ANS** in both gel and sol states. Since the emission was stronger in gel and sol than in pure water, it was clear that **PalG₃H** formed a micelle-like assembly.

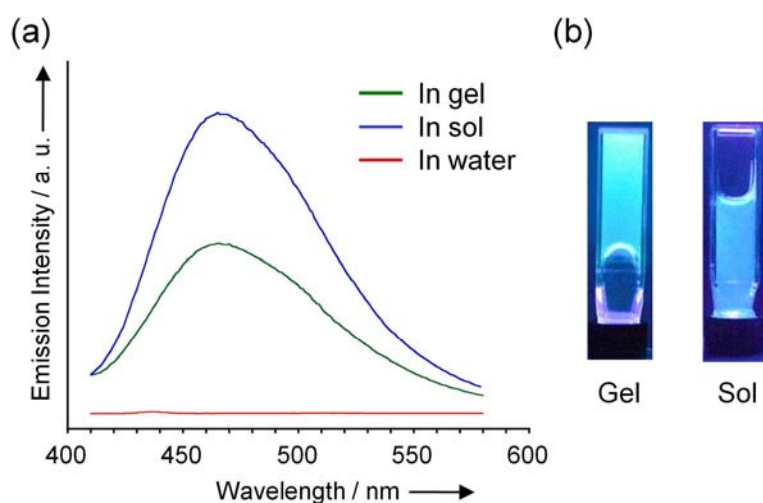


Figure S8 Fluorescence spectra (a) and photographs (b, under UV lamp with a wavelength of 365 nm) of **ANS**-containing gel and sol. [**ANS**] = 1 μ M in water, [**PalG₃H**] = 0.2 wt% and λ_{ex} = 380 nm.

5. Fourier-Transform Infrared Spectroscopy

PalG₃H with a weight of 10 mg was well-dispersed into 1 mL of D₂O by sonication for 10 min, and then, this dispersion was kept for 10 min at 363 K or 333 K, to prepare gel and sol. Also, the DMSO-*d*₆ solution of **PalG₃H** solution with the same concentration was prepared as a reference sample. The samples were sandwiched between CaF₂ windows with a 0.5 mm gap. The Fourier-transform infrared (FT-IR) spectra were recorded with a FT/IR-620 spectrometer (JASCO Co.) equipped with a TGS detector. All spectra were obtained with a resolution of 2 cm⁻¹ and 64 scans at 298 K.

Figure S9 shows FT-IR spectra of **PalG₃H** in the D₂O gel, the D₂O sol and the DMSO-*d*₆ solution. For the D₂O gel, the symmetric and antisymmetric C-H stretching vibrations of CH₂ groups were observed at 2849 cm⁻¹ and 2919 cm⁻¹, respectively. These values were smaller than those obtained for the DMSO-*d*₆ solution, in which **PalG₃H** was molecularly dispersed. This indicates that the alkyl chain in **PalG₃H** are ordered in the gel state.⁶ Also, the absorption peak assignable to the C=O stretching vibration, namely amide I band, were splitted at 1645 cm⁻¹ and 1632 cm⁻¹ for the D₂O gel. On the contrary, the DMSO-*d*₆ solution gave the corresponding absorption peak at 1670 cm⁻¹, including the contribution from trifluoroacetate.⁷ Such a red-shift of amide I band is characteristic of a hydrogen bonding.^{8,9} Importantly, there was no substantial difference between FT-IR

spectra for the gel and sol. Thus, it can be claimed that **PalG₃H** formed a micelle-like assembly, which was accompanied by the alkyl-chain ordering and hydrogen bonding both in the gel and sol states.

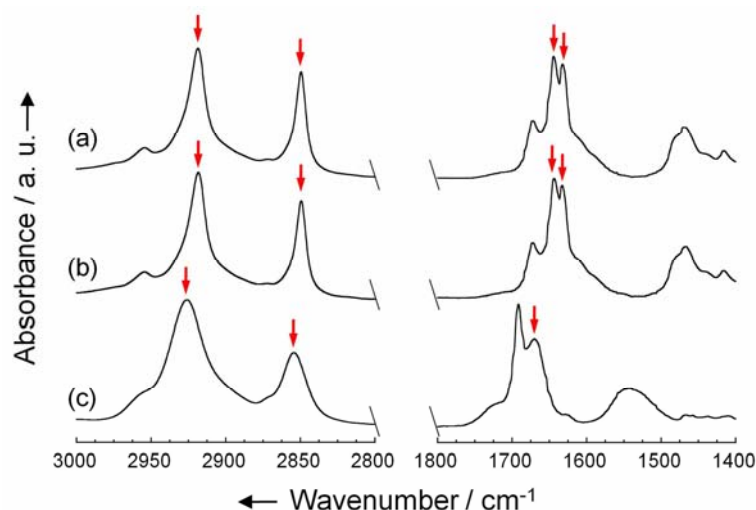


Figure S9 Partial FT-IR spectra of **PalG₃H** in the gel (a, D₂O), the sol (b, D₂O) and the solution states (c, DMSO-*d*₆) at 298 K. [**PalG₃H**] = 1.0 wt%.

6. References

- S1 D. Koda, T. Maruyama, N. Minakuchi, K. Nakashima and M. Goto, *Chem. Commun.*, 2010, **46**, 979.
- S2 J. T. Finer, R. M. Simmons and J. A. Spudich, *Nature*, 1994, **368**, 113.
- S3 M. Salomo, R. K. Kegler, C. Gutsche, M. Struhalla, J. Reinmuth, W. Skokow, U. Hahn and F. Kremer, *Colloid Polym. Sci.*, 2006, **284**, 1325.
- S4 D. Velegol and F. Lanni, *Biophys. J.*, 2001, **81**, 1786.
- S5 M. A. Greenfield, J. R. Hoffman, M. O. Olvera and S. I. Stupp, *Langmuir*, 2010, **26**, 3641.
- S6 A. N. Parikh, D. L. Allara, I. B. Azouz and F. Rondelez, *J. Phys. Chem.*, 1994, **98**, 7577.
- S7 L. E. Valenti, M. B. Paci, C. P. DePauli and C. E. Giacomelli, *Anal. Biochem.*, 2011, **410**, 118.
- S8 N. Yamada, K. Ariga, M. Naito, K. Matsubara and E. Koyama, *J. Am. Chem. Soc.*, 1998, **120**, 12192.
- S9 J. P. Schneider, D. J. Pochan, B. Ozbas, K. Rajagopal, L. Pakstis and J. Kretsinger, *J. Am. Chem. Soc.*, 2002, **124**, 15030.